The yeast DASH complex forms closed rings on microtubules

JJ L Miranda[1], Peter De Wulf[2], Peter K Sorger[2,3] & Stephen C Harrison[4]

The *Saccharomyces cerevisiae* DASH complex is an essential microtubule-binding component of the kinetochore. We coexpressed all ten subunits of this assembly in *Escherichia coli* and purified a single complex, a ~210-kDa heterodecamer with an apparent stoichiometry of one copy of each subunit. The hydrodynamic properties of the recombinant assembly are indistinguishable from those of the native complex in yeast extracts. The structure of DASH alone and bound to microtubules was visualized by EM. The free heterodecamer is relatively globular. In the presence of microtubules, DASH oligomerizes to form rings and paired helices that encircle the microtubules. We discuss potential roles for such collar-like structures in maintaining microtubule attachment and spindle integrity during chromosome segregation.

Chromosome segregation requires the attachment of spindle microtubules (MTs) to kinetochores, multiprotein complexes that assemble on centromeric DNA. Faithful segregation also requires that sister chromatids establish bipolar MT attachments in which one kinetochore binds a MT emanating from one spindle pole and the sister kinetochore binds a MT emanating from the opposite pole. Kinetochores remain bound to the ends of growing and shrinking MTs and can transduce energy released by MT depolymerization into pulling forces. Bipolar kinetochore-MT attachment imposes sufficient tension on sister chromatids to stretch centromeric chromatin during metaphase and disjoin chromatids at anaphase.

Kinetochore architecture is best understood in the budding yeast *S. cerevisiae*, which has the smallest known centromeres. *Saccharomyces cerevisiae* kinetochores contain 60 or more protein subunits organized into at least 14 distinct multiprotein complexes[1]. The entire assembly forms a bridge between the DNA of a centromere and a single spindle MT. Dam1p, a MT-binding component of yeast kinetochores that also localizes to spindle MTs[2–5], is part of a ten-protein complex, variously called Dam1 complex or DASH, which also contains Duo1p, Dad1p, Dad2p, Spc19p, Spc34p, Ask1p, Dad3p, Dad4p and Hsk3p[6–10]. All ten are essential proteins. Mutations in DASH subunits prevent the formation and maintenance of bipolar kinetochore-MT attachments[7,11] and destabilize the spindle[2–10,12]. Ipl1p, a spindle assembly checkpoint kinase required for resolving syntelic kinetochore-MT attachments formed early in mitosis[13], seems to regulate association of DASH with other kinetochore complexes[9,14], suggesting a possible mechanism for the establishment of bipolarity.

DASH isolated from yeast binds MTs[6]. Understanding how it does so may help explain how kinetochores attach to the spindle and how these attachments are maintained during rounds of MT polymerization and depolymerization. We have produced DASH by recombinant methods in *E. coli* and examined its structural properties using EM. We find that DASH forms a ring-like structure that encircles MTs. This collar might be one component of a proposed sleeve that has been suggested on theoretical grounds as a means by which kinetochores could hold onto dynamic MTs[15].

RESULTS

Recombinant coexpression

Attempts to express individual components of DASH in *E. coli* as soluble proteins for reconstitution were largely unsuccessful. Rather than conducting refolding experiments, we attempted coexpression of the entire complex. A modular approach using a polycistronic vector has been successful for coexpression of the three-protein VHL–elongin C–elongin B complex from one bacterial plasmid[16]. To accommodate the ten subunits of DASH, we enhanced that system by constructing new vectors that increase the capacity of each polycistron to five open reading frames (ORFs) and allow the transcription of two messages from one plasmid. One of the ten subunits was fused to a C-terminal His$_6$-tag to facilitate purification. All ten subunits were coexpressed from one vector (**Supplementary Fig. 1** online), and the resulting assembly was purified by metal affinity, ion exchange, and gel filtration chromatography. *Escherichia coli* DnaK, a common chaperone contaminant in bacteria[17], binds to the complex during purification, and a competitor peptide[18] was added at multiple steps in the preparation to release the chaperone. We obtained ~0.1–0.2 mg of purified DASH from each liter of bacterial culture.

Purified, recombinant DASH is a heterodecamer containing the ten expressed proteins (**Supplementary Fig. 1** online). In complexes

[1]Department of Molecular and Cellular Biology, Harvard University, Cambridge, Massachusetts 02138, USA. [2]Department of Biology and [3]Biological Engineering Division, Massachusetts Institute of Technology, Cambridge, Massachusetts 02139, USA. [4]Department of Biological Chemistry and Molecular Pharmacology and Howard Hughes Medical Institute, Harvard Medical School, Boston, Massachusetts 02115, USA. Correspondence should be addressed to S.C.H. (harrison@crystal.harvard.edu).
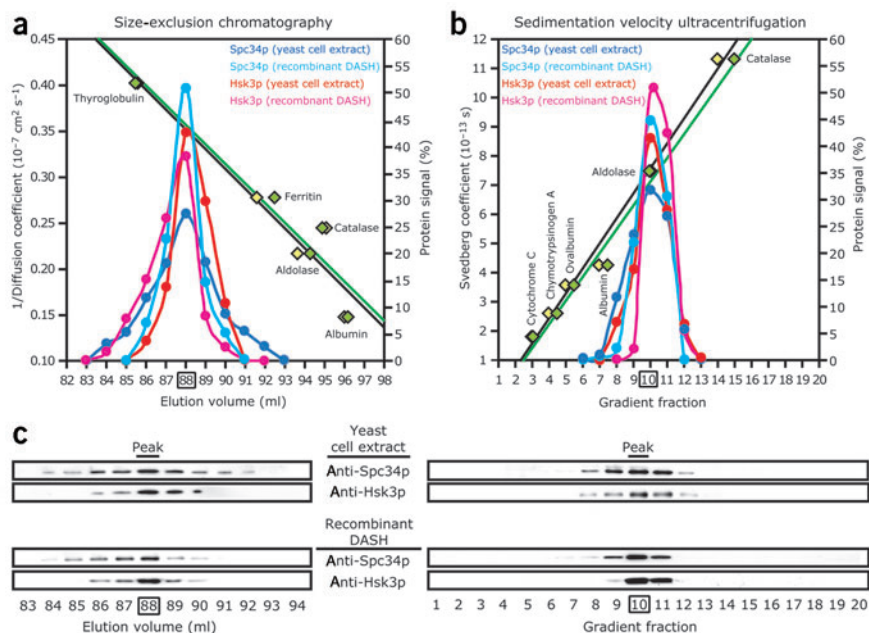
Figure 1 Hydrodynamic analysis of recombinant and native DASH. (**a**) Elution profiles from size-exclusion chromatography. Yellow and green diamonds, elution positions of five standard proteins as obtained from two independent experiments. Black and green regression lines (r^2 = 0.91 and 0.92, respectively) yield the diffusion coefficient of a protein from its elution volume. (**b**) Sedimentation profiles from sedimentation velocity ultracentrifugation. Yellow and green diamonds, sedimentation positions of six standard proteins as obtained from two independent experiments. Black and green regression lines (r^2 = 0.98, and 0.99, respectively) yield the Svedberg coefficient of a protein from its position in the glycerol gradient. (**c**) Western blots of column and gradient fractions obtained with polyclonal antibodies raised against Spc34p and Hsk3p. Quantitation of the band intensity is plotted in **a** and **b**.

containing His$_6$-tagged Dad1p, all ten components resolved well on SDS-polyacrylamide gels stained with colloidal Coomassie blue, and densitometry suggested that each subunit is present at equimolar stoichiometry. Substoichiometric bands, one below Duo1p and two below Dad1p, were identified by mass spectrometry as degradation products of components of the complex. Coexpression of all ten subunits seems necessary for formation of complex. For example, in the absence of Hsk3p, two separate subcomplexes form, one comprising Ask1p, Dad2p and Dad4p, and the other comprising Dad1p, Dad3p, Dam1p, Duo1p, Spc19p and Spc34p (data not shown). All results presented here were obtained with DASH containing His$_6$-tagged Spc34p, but these were reproduced with preparations containing a His$_6$-tag on different component proteins (data not shown).

Heterodecamer characterization

To compare recombinant and native DASH, we carried out size-exclusion chromatography and sedimentation velocity ultracentrifugation with our purified preparations and whole-cell yeast extracts side by side (**Fig. 1**). Fractionation of DASH was traced by western hybridization using antibodies generated against Spc34p and Hsk3p. Sedimentation equilibrium ultracentrifugation and gel filtration chromatography indicate a tendency for recombinant DASH to aggregate in a concentration-, salt-, and pH-dependent manner (data not shown), but aggregation could be reduced substantially at dilute concentrations. At ~1–10 μM, the diffusion coefficient, $2.8 \pm 0.1 \times 10^{-7}$ cm^2 s^{-1}, and sedimentation coefficient, $7.4 \pm 0.3 \times 10^{-13}$, of the complex yield a calculated molecular mass of 211 ± 16 kDa, consistent with the predicted molecular mass of 204 kDa, assuming one copy of each subunit and one His$_6$-tag.

The Stokes radius of 76 ± 2 Å is larger than 40 and 50 Å, the ideal minimum and experimentally expected radii, respectively, for a 200-kDa protein. The calculated frictional coefficient of 1.90 ± 0.03 suggests either an elongated shape or the presence of unstructured extensions. The hydrodynamic properties of the recombinant and native complexes were indistinguishable, arguing that recombinant DASH is similar to the complex present *in vivo*.

EM of rotary shadowed recombinant DASH revealed the presence of globular species, often oblong rather than circular, and sometimes triangular (**Fig. 2**). Each particle is ~170 ± 20 Å (*n* = 116) in diameter without correction for the platinum-carbon grain size, which we estimate as 20 Å on all sides. Thus, EM and hydrodynamic measurements yield similar diameters for the complex, 130 and 150 Å, respectively. Both techniques show that the heterodecamer is relatively globular in solution.

Microtubule decoration

Recombinant DASH cosediments with paclitaxel-stabilized MTs (**Supplementary Fig. 2** online), and the decorated MTs have a characteristic appearance when visualized by negative staining EM. Whereas MTs alone appear as ~250 Å–wide fibers (**Fig. 3a**), MTs decorated with DASH have prominent transverse striations (**Fig. 3b**). The striations are more or less perpendicular to the MT axis, although the tilt of successive striations varies slightly, as does axial spacing. Each striation appears as a continuously contrasted mass, 50 ± 10 Å (*n* = 117 from seven MTs) thick and 480 ± 30 Å (*n* = 267 from ten MTs) in diameter. The striations extend 110 ± 10 Å (*n* = 267 from ten MTs) beyond the MT on each side. Their diameter varies slightly, depending on the degree of MT flattening, and perhaps on the number of MT protofilaments and the angle relative to the MT axis. The termination points of striations are not seen, arguing against the binding of extended, linear species to MTs. Thus, the observed bands represent the projection of either a closed circular ring or a filamentous helix.
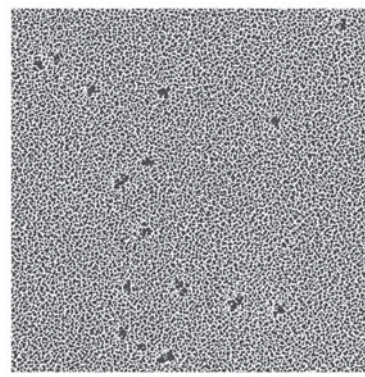

Figure 2 Electron micrograph of a representative field of DASH heterodecamers shadowed with platinum. Scale bar, 250 Å.
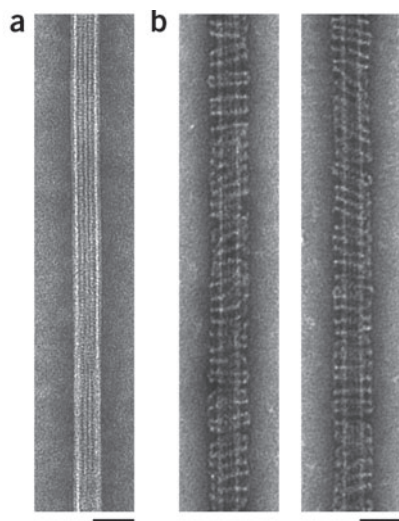
Figure 3 Decoration of MTs with DASH. (**a**,**b**) Gallery of negatively stained MTs in the (**a**) absence and (**b**) presence of DASH. Scale bars, 500 Å.

By varying the ratio of DASH to tubulin, we could alter the number of and spacing between striations on each MT and obtain further details of the binding mode. At a 1:10 molar ratio of DASH to tubulin heterodimer, isolated striations could be observed (**Fig. 4a**). In certain cases, the contrasted structure could be followed along the edge of a MT and even around its complete circumference, revealing a single closed ring. The radial thickness of the ring appeared to be similar to the thickness of the striations perpendicular to the MT axis, leaving ~60 Å between the outer diameter of the MT and the inner diameter of the ring. Negative stain did not reveal any clear mass of protein directly bridging the MT and the ring. Based on the diameter of the ring and the dimensions of the heterodecamer obtained by hydrodynamic analysis and rotary shadowing measurements, we estimate that the number of heterodecamers required to fully encircle a MT is between 10 and 15. MTs polymerized *in vitro* under our conditions predominantly contain 13–15 protofilaments, and MTs *in vivo* contain 13 protofilaments. The actual binding stoichiometry could therefore correspond to one heterodecamer per MT protofilament.

Adjacent striations tend to pair with similar tilts relative to the MT axis when the MT is saturated with DASH. Examination of decorated MTs at equimolar concentrations of DASH and tubulin heterodimer sometimes reveals the presence of paired helices, a structural variation of a ring (**Fig. 4b**). The path of these helices could also be traced around the circumference of the MT. The spacing between paired strands is 100 ± 10 Å ($n = 69$ from 13 helical stretches on 9 MTs), slightly longer than the spacing corresponding to the tubulin heterodimer repeat, and the helical pitch is 250 ± 20 Å ($n = 13$ helical stretches from 9 MTs).

Tubulin itself can form both rings and spirals around MTs in the presence of polycations[19–22]. Immunogold labeling experiments show that the decoration we observe is indeed DASH, not tubulin. We used a monoclonal primary antibody specific for the C-terminal His$_6$-tag, which was on Spc34p. In the presence of this antibody, protein A conjugated to 5-nm gold particles localized specifically to rings on the MTs (**Fig. 5a**), and undecorated MTs remained unlabeled. We also observed frequent pairing of rings in this experiment, a result consistent with crosslinking by bivalent antibodies. In the absence of primary antibody, we detected no selective gold localization (**Fig. 5b**).

DISCUSSION
Mode of microtubule binding

We have shown that DASH is a relatively globular heterodecamer in solution that oligomerizes in the presence of MTs to form closed rings and paired helices that encircle the MTs (**Fig. 6**). Rings and helices do not form in the absence of MTs, suggesting that MT binding is necessary for ring and helix formation and that the MTs template or seed this assembly. Rings form even at low molar ratios of DASH relative to tubulin, suggesting that ring formation is cooperative, with completion of a ring being more favorable than initiation of a new ring. MT encirclement by DASH is distinct from the modes of binding observed for other MT-associated proteins. MAP2 and tau contain three or four intramolecular repeats of a MT-binding motif that bind to successive tubulin heterodimers longitudinally along a protofilament[23]. In the case of kinesin-like proteins, each motor domain binds a single tubulin heterodimer[24], but kinesin dimers span adjacent tubulin heterodimers, also longitudinally along a protofilament[25]. MAP2, tau and kinesin do not oligomerize laterally to form closed rings or filaments.

In negatively stained preparations, there is a gap between the MT and DASH rings or helices that is not spanned by any strongly contrasted structure. Flattening of the decorated MT may artificially enhance this property, but we find that the diameters of striations observed on MTs in vitreous ice, where flattening does not occur, is similar (data not shown). The lack of a large contact area may be explained by a binding interface consisting of extensions of a flexible peptide rather than a globular domain. Such extensions might not be detected in images of negatively stained samples. DASH decorates subtilisin-cleaved MTs in a manner similar to untreated MTs (data not shown), suggesting that the flexible C termini of tubulin subunits are not essential for binding. The binding interface may thus consist
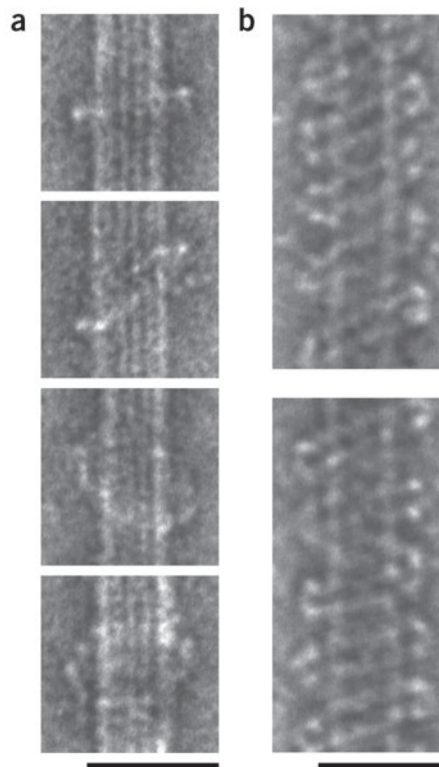

Figure 4 Different modes of MT decoration by DASH. (**a**,**b**) Gallery of negatively stained MTs in the presence of DASH showing (**a**) single rings and (**b**) paired helices. Scale bars, 500 Å.
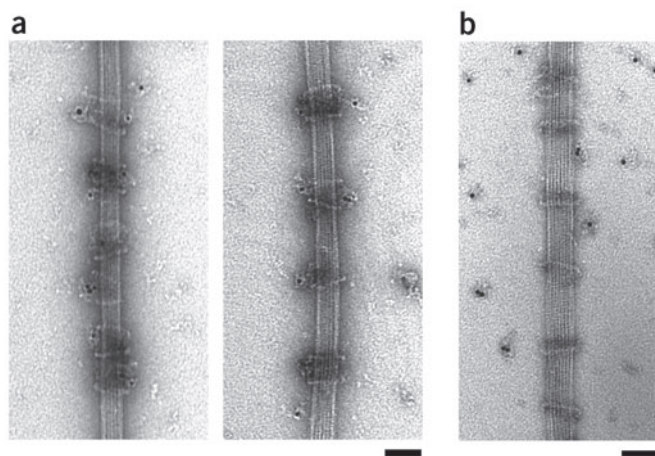
Figure 5 Immunogold labeling of MTs decorated with DASH. (**a**) Decorated MTs incubated with monoclonal anti-His (C-terminal) and protein A conjugated with 5-nm gold particles. (**b**) Decorated MTs incubated with only protein A conjugated with 5-nm gold particles. Scale bars, 500 Å.

of extended polypeptide projecting from DASH associated with the globular core of tubulin.

Formation of both rings and helices by DASH on MTs is consistent with a ring-to-lockwasher transition as seen in some symmetrical, oligomeric assemblies. The helicase domain of the bacteriophage T7 helicase-primase crystallizes as both a hexameric ring with $P6$ symmetry and a helical filament with $P6_1$ symmetry[26,27]. The GTPase dynamin self-assembles into oligomers of both rings and helices *in vitro*[28]. In the case of DASH, helices represent a propagated, ordered state of the ring, but are only observed at high binding stoichiometry *in vitro*. The lack of obvious contacts between adjacent rings and the observation of single rings at low molar ratios of DASH relative to tubulin suggest that the ring is the basic architectural unit of the assembly on MTs.

Genome-wide analysis of yeast protein abundance estimates the copy number of seven DASH components at ~1,000 per cell[29], and our own quantitative western blotting experiments calibrated by protein A yield an estimated 650 ± 50 copies of TAP-tagged Dam1p per cell, corresponding to ~1 µM (data not shown). At this concentration, an average of one or two rings could form on each of the 32 kinetochore MTs and 8 interpolar MTs in haploid yeast. This arithmetic suggests that helices are unlikely to form *in vivo*, and we therefore propose that rings are the biologically functional unit of DASH assembly on MTs.

Implications for kinetochore function

Loss of functional DASH prevents kinetochores from forming and maintaining stable bipolar attachments to MTs, and destabilizes the spindle. Imaging of yeast cells show the complex primarily at kinetochores, with some additional localization on part of the spindle[11]. If each MT contains only one or two rings, however, DASH cannot function by coating the length of the MT. Instead, DASH may function primarily at the (+)-ends of MTs. MAP2 and tau are thought to protect MTs against depolymerization by bridging tubulin subunits longitudinally and stabilizing the straight form of the protofilament, thus preventing the transition to the curved, depolymerizing form[23]. Doublecortin is thought to stabilize interactions both longitudinally between tubulin monomers and laterally between protofilaments by providing additional contacts in a fenestration between four tubulin monomers[30]. DASH may function similarly by encircling MTs and laterally bridging protofilaments, thereby stabilizing interprotofila-
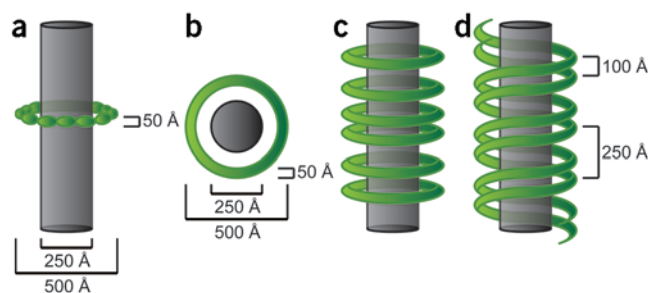
ment association and constraining the bending and splaying that occurs at depolymerizing ends.

The presence of a ring-like structure at the kinetochore has implications for the mechanism of kinetochore-MT attachment. During metaphase and anaphase, kinetochores must remain bound to the (+)-ends of dynamic MTs, a process that is topologically challenging. The presence of a sleeve has been proposed previously as a mechanical solution for this problem[15]. DASH collars at the kinetochore could be part of such a sleeve. Because depolymerization at the MT (+)-end proceeds by protofilament splaying, a ring will be retained on the MT and induced to slide longitudinally, ensuring sustained attachment and helping to couple depolymerization to translation. In DNA metabolism, protein rings that slide along DNA confer processivity to different functions that require prolonged tracking[31]. The ring-like structures provide a topological link with DNA, maintaining attachment even as DNA is polymerized, unwound or depolymerized. The same structural solution may have evolved for the problem of MT attachment. In the absence of a stable MT collar, kinetochores might retain their ability to capture MTs, but attachment would be weaker and subject to breakage. Mutations in DASH subunits indeed produce such effects *in vivo*.

METHODS

Plasmids. A modular system for coexpression of four proteins in bacteria from a single polycistron[16] was modified to coexpress ten proteins from two polycistrons on the same plasmid. The sequence GAGCTCCAATTGGAATTCGCTAGC was inserted between the MluI and XbaI sites of pET21a+ (Novagen) to generate pET21aTr. This new transfer vector allows insertion of a fifth ORF between the MluI and XhoI sites of pST39. The sequence GACCTGCTAGCATGACTGGTG GACAGAAATGGGTCTGCAGCG was inserted into the RsrII site of pST39 to generate pST39Dual. This plasmid serves as the new backbone for coexpression. One polycistron containing five ORFs from pST39 may be inserted as a NsiI-SpeI fragment into the new PstI and NheI sites. A second polycistron containing another five ORFs from a different pST39 plasmid may then be inserted between the original NsiI and SpeI sites. The two polycistrons are antiparallel to one another and under the control of separate T7 promoters and terminators.

Cloning. DASH component genes were cloned from *S. cerevisiae* W303 and inserted into PCR4Blunt-TOPO (Invitrogen) with flanking NdeI and BamHI sites. Silent mutations were introduced to remove internal NdeI and BamHI sites using the QuikChange site-directed mutagenesis kit (Stratagene), and all genes were subcloned into pET3aTr as NdeI-BamHI fragments. Additional mutagenesis to remove restriction sites necessary for further subcloning was carried out in pET3aTr. *ASK1* and *HSK3* were subcloned into pET21aTr as NdeI-BamHI fragments. One polycistron was constructed as follows: *DAD4*, *DAD3* and *DAD2* were sequentially subcloned from pET3aTr into the compatible restriction sites of the first three cassettes in pST39 as NheI-BamHI, EcoRI-HindIII, and SacI-KpnI

Figure 6 Schematic model of MTs decorated with DASH. (**a**) A single ring viewed orthogonal to the MT axis as seen in electron micrographs. (**b**) A single ring viewed along the MT axis. (**c**,**d**) Multiple rings (**c**) and a paired helix (**d**) viewed orthogonal to the MT axis.

fragments, respectively. *SPC19* from pET3aTr as a BspEI-MluI fragment and *ASK1* from pET21aTr as a MluI-XhoI fragment were inserted into BspEI-XhoI-digested pST39 containing *DAD4*, *DAD3* and *DAD2*. The second polycistron was constructed in a similar fashion. *DAD1* was subcloned from pET3aTr into the first cassette of pST39 as a XbaI-BamHI fragment. *DUO1* was subcloned from pET3aTr to the second cassette of a different pST39 plasmid as a MfeI-HindIII fragment, and then inserted as a BsrGI-HindIII fragment into BsrGI-HindIII-digested pST39 containing *DAD1*. *SPC34* was subcloned from pET3aTr into the third cassette of pST39 containing *DAD1* and *DUO1* as a SacI-KpnI fragment. *DAM1* from pET3aTr as a BspEI-BssHII fragment and *HSK3* from pET21aTr as a MluI-XhoI fragment were inserted into BspEI-XhoI-digested pST39 containing *DAD1*, *DUO1*, and *SPC34*. The *DAD4/DAD3/DAD2/SPC19/ASK1* polycistron was inserted into NheI-PstI-digested pST39Dual as a NsiI-SpeI fragment. The *DAD1/DUO1/SPC34/DAM1/HSK3* poycistron was inserted as a NsiI-SpeI fragment into NsiI-SpeI-digested pST39Dual containing the other polycistron. This procedure was repeated to generate similar plasmids with *ASK1*, *DAD1*, *DAD2*, *DAD3*, *DAD4*, *HSK3*, *SPC19* and *SPC34* encoding a C-terminal His$_6$-tag.

Expression and purification. Coexpression plasmids were transformed into *E. coli* BL21-AI (Invitrogen) harboring the pRARE plasmid (Novagen) and grown for 3–5 h at 37 °C after induction with 0.2% (w/v) arabinose at an A_{600} of 0.4. Cells were lysed in 50 mM phosphate, 500 mM NaCl, 20 mM imidazole, 5 mM mercaptoethanol, 1 mM PMSF and Complete protease inhibitors without EDTA (Roche), pH 7.5. The supernatant was bound to Ni-NTA agarose (Qiagen), washed in the same buffer without protease inhibitors, and eluted with 200 mM imidazole. The eluant was exchanged into 50 mM phosphate, 25 mM NaCl, 1 mM mercaptoethanol, 1 mM EDTA, pH 7.5 by concentration. ATP was added to 1 mM and the synthetic peptide NRLLLTG was added to 250-fold molar excess relative to the DASH. The mixture was incubated for 1 h and purified on a MonoQ 5/50 column (Amersham) with a gradient of 25–415 mM NaCl. The eluant was concentrated, mixed with ATP and the NRLLLTG peptide again, and purified on a Superose 6 10/300 column (Amersham) equilibrated in 25 mM HEPES, 500 mM NaCl, 1 mM mercaptoethanol, 1 mM EDTA, pH 7.4. All steps were carried out at 4 °C.

Antibody production. pET3aTr plasmids containing *SPC34* or *HSK3* encoding a C-terminal His$_6$-tag were transformed into *E. coli* BL21-AI (Invitrogen) harboring the pRARELysS plasmid (Novagen) and grown as described above. Cells were lysed in the same buffer supplemented with 1% (v/v) Triton X-100. The pellet was washed three times in buffer without protease inhibitors and redissolved in buffer with 6 M guanidine substituting for 1% (v/v) Triton X-100. The supernatant was bound to Ni-NTA agarose (Qiagen), washed in the same buffer, and eluted with 200 mM imidazole. The eluant was injected into rabbits for the production of polyclonal antibodies (Covance).

Hydrodynamic analysis. Size-exclusion chromatography was carried out on a HiPrep 16/60 Sephacryl S-500 HR column (Amersham) equilibrated in 100 mM bis-tris-propane, 150 mM KCl, 10 mM EDTA, 50 mM β-glycerophosphate, pH 7.5 at 4 °C. Calibration was done with the known diffusion constants[32,33] of thyroglobulin, ferritin, catalase, aldolase and albumin (Amersham, Boehringer Mannheim). *Saccharomyces cerevisiae* W303 was grown in YPD to an A_{600} of 1.0–1.2, spun down, and ground in liquid nitrogen with mortar and pestle[34]. Total cell extract protein (500 μg) or recombinant DASH (750 ng) was loaded onto the column. Fractions of 1 ml were collected, precipitated with 1 M trichloroacetic acid, rinsed with acetone, and examined by western blotting using 1:750 dilutions of polyclonal anti-Spc34p or anti-Hsk3p. Sedimentation velocity ultracentrifugation was done with a 10%–40% (v/v) 5-ml glycerol density gradient made in size-exclusion buffer and layered in 13 × 51 mm open-top Polyclear centrifuge tubes (Seton Scientific) using the Biocomp Gradient Master (Biocomp Instruments). Yeast extract was made as described above, and 150 μg total cell extract protein or 750 ng recombinant DASH was loaded onto the gradient. The gradients were centrifuged at 370,000*g* for for 12 h at 4 °C in a SW55Ti swinging bucket rotor and Optima L-80 Ultracentrifuge (Beckman Instruments). Fractionation was carried out robotically using a Biocomp Piston Gradient Fractionator (Biocomp Instruments, version 5.60) by removing 20 fractions of 1.9 mm from the top. Calibration was done with the known sedimentation constants[35] of ribonuclease A, chymotrypsinogen A, ovalbumin, albumin, aldolase and catalase (Amersham). The Stokes radius, molecular mass and frictional coefficient of DASH was determined using the Stokes-Einstein equation.

Microtubule decoration. Bovine tubulin (Cytoskeleton) was polymerized at 5 mg ml^{-1} in 74 mM PIPES, 1 mM GTP, 1 mM MgCl$_2$, 1 mM EGTA, 100 μM paclitaxel, 5–7.5% (v/v) DMSO, pH 6.9 for 30 min at 35 °C. MTs were diluted to 0.055 mg ml^{-1} in 25 mM HEPES, 100 mM NaCl, 1 mM GTP, 10 μM paclitaxel, 1% (v/v) DMSO, pH 7.4. Binding was carried out by diluting 5 μl of 1 mg ml^{-1} DASH with 45 μl of MT solution. Control samples were treated with buffer instead of DASH. All samples were incubated for 20 min at room temperature. Partial decoration for observation of single rings was achieved by diluting the DASH concentration in the reaction ten-fold. Immunogold labeling was done by adding 0.3 μl of 1.2 mg ml^{-1} monoclonal anti-His (C-terminal) (Invitrogen) and 0.6 μl of protein A conjugated with 5-nm gold particles (University of Utrecht) at A_{520} of 6 to partially decorated microtubules. Control samples were treated with buffer instead of monoclonal antibody. All samples were incubated for an additional 20 min at room temperature.

Electron microscopy. Negatively stained preparations were made by adsorbing decorated MTs onto freshly glow-discharged grids coated with parlodion and carbon. In some cases with 0.1 mg ml^{-1} DASH, the sample was spun at 18,000*g* for 10 min at room temperature and resuspended in the same buffer before adsorption to reduce protein background. The grid was washed and stained with 0.7% (w/v) uranyl formate. For rotary shadowing experiments, 0.1 to 0.5 mg ml^{-1} DASH was diluted five-fold into 112 mM ammonium bicarbonate, 45% (v/v) glycerol, pH 7.5, sprayed onto freshly cleaved mica, dried, and shadowed with platinum. Images of negatively stained and rotary shadowed samples were obtained on a JOEL-1200EX microscope operating at 80 kV with a nominal magnification of 30,000× and 45,000×, respectively. Measurements were taken on digitized negatives with distances calibrated by replica gratings (Electron Microscopy Sciences).

Note: Supplementary information is available on the Nature Structural & Molecular Biology website.

1. McAinsh, A.D., Tytell, J.D. & Sorger, P.K. Structure, function, and regulation of budding yeast kinetochores. *Annu. Rev. Cell Dev. Biol.* **19**, 519–539 (2003).
2. Hofmann, C. *et al.* *Saccharomyces cerevisiae* Duo1p and Dam1p, novel proteins involved in mitotic spindle function. *J. Cell Biol.* **143**, 1029–1040 (1998).
3. Jones, M.H., Bachant, J.B., Castillo, A.R., Giddings, T.H. Jr. & Winey, M. Yeast Dam1p is required to maintain spindle integrity during mitosis and interacts with the Mps1p kinase. *Mol. Biol. Cell* **10**, 2377–2391 (1999).
4. Cheeseman, I.M., Enquist-Newman, M., Muller-Reichert, T., Drubin, D.G. & Barnes, G. Mitotic spindle integrity and kinetochore function linked by the Duo1p/Dam1p complex. *J. Cell Biol.* **152**, 197–212 (2001).
5. Jones, M.H., He, X., Giddings, T.H. & Winey, M. Yeast Dam1p has a role at the kinetochore in assembly of the mitotic spindle. *Proc. Natl. Acad. Sci. USA* **98**, 13675–13680 (2001).
6. Cheeseman, I.M. *et al.* Implication of a novel multiprotein Dam1p complex in outer kinetochore function. *J. Cell Biol.* **155**, 1137–1145 (2001).
7. Janke, C., Ortiz, J., Tanaka, T.U., Lechner, J. & Schiebel, E. Four new subunits of the Dam1-Duo1 complex reveal novel functions in sister kinetochore biorientation. *EMBO J.* **21**, 181–193 (2002).
8. Li, Y. *et al.* The mitotic spindle is required for loading of the DASH complex onto the kinetochore. *Genes Dev.* **16**, 183–197 (2002).
9. Cheeseman, I.M. *et al.* Phospho-regulation of kinetochore-microtubule attachments by the Aurora kinase Ipl1p. *Cell* **111**, 163–172 (2002).
10. Li, J., Li, Y. & Elledge, S.J. Genetic analysis of the kinetochore DASH complex reveals an antagonistic relationship with the ras/protein kinase A pathway and a novel subunit required for Ask1 association. *Mol. Cell. Biol.* **25**, 767–778 (2005).

11. He, X., Rines, D.R., Espelin, C.W. & Sorger, P.K. Molecular analysis of kinetochore-microtubule attachment in budding yeast. *Cell* **106**, 195–206 (2001).

12. Enquist-Newman, M. *et al.* Dad1p, third component of the Duo1p/Dam1p complex involved in kinetochore function and mitotic spindle integrity. *Mol. Biol. Cell* **12**, 2601–2613 (2001).

13. Tanaka, T.U. *et al.* Evidence that the Ipl1-Sli15 (Aurora kinase-INCENP) complex promotes chromosome bi-orientation by altering kinetochore-spindle pole connections. *Cell* **108**, 317–329 (2002).

14. Shang, C. *et al.* Kinetochore protein interactions and their regulation by the Aurora kinase Ipl1p. *Mol. Biol. Cell* **14**, 3342–3355 (2003).

15. Hill, T.L. Theoretical problems related to the attachment of microtubules to kineto-chores. *Proc. Natl. Acad. Sci. USA* **82**, 4404–4408 (1985).

16. Tan, S. A modular polycistronic expression system for overexpressing protein complexes in *Escherichia coli. Protein Expr. Purif.* **21**, 224–234 (2001).

17. Rial, D.V. & Ceccarelli, E.A. Removal of DnaK contamination during fusion protein purifications. *Protein Expr. Purif.* **25**, 503–507 (2002).

18. Gragerov, A., Zeng, L., Zhao, X., Burkholder, W. & Gottesman, M.E. Specificity of DnaK-peptide binding. *J. Mol. Biol.* **235**, 848–854 (1994).

19. Jacobs, M., Bennett, P.M. & Dickens, M.J. Duplex microtubule is a new form of tubulin assembly induced by polycations. *Nature* **257**, 707–709 (1975).

20. Behnke, O. An outer component of microtubules. *Nature* **257**, 709–710 (1975).

21. Erickson, H.P. & Voter, W.A. Polycation-induced assembly of purified tubulin. *Proc. Natl. Acad. Sci. USA* **73**, 2813–2817 (1976).

22. Erickson, H.P. Facilitation of microtubule assembly by polycations. In *Cell Motility* Vol. 3 (eds. Goldman, R., Pollard, T. & Rosenbaum, J.) 1069–1080 (Cold Spring Harbor Laboratory, Cold Spring Harbor, New York, 1976).

23. Al-Bassam, J., Ozer, R.S., Safer, D., Halpain, S. & Milligan, R.A. MAP2 and tau bind longitudinally along the outer ridges of microtubule protofilaments. *J. Cell Biol.* **157**, 1187–1196 (2002).

24. Kikkawa, M., Ishikawa, T., Wakabayashi, T. & Hirokawa, N. Three-dimensional structure of the kinesin head-microtubule complex. *Nature* **376**, 274–277 (1995).

25. Hoenger, A. *et al.* A new look at the microtubule binding patterns of dimeric kinesins. *J. Mol. Biol.* **297**, 1087–1103 (2000).

26. Sawaya, M.R., Guo, S., Tabor, S., Richardson, C.C. & Ellenberger, T. Crystal structure of the helicase domain from the replicative helicase-primase of bacteriophage T7. *Cell* **99**, 167–177 (1999).

27. Singleton, M.R., Sawaya, M.R., Ellenberger, T. & Wigley, D.B. Crystal structure of T7 gene 4 ring helicase indicates a mechanism for sequential hydrolysis of nucleotides. *Cell* **101**, 589–600 (2000).

28. Hinshaw, J.E. & Schmid, S.L. Dynamin self-assembles into rings suggesting a mechanism for coated vesicle budding. *Nature* **374**, 190–192 (1995).

29. Ghaemmaghami, S. *et al.* Global analysis of protein expression in yeast. *Nature* **425**, 737–741 (2003).

30. Moores, C.A. *et al.* Mechanism of microtubule stabilization by doublecortin. *Mol. Cell* **14**, 833–839 (2004).

31. Hingorani, M.M. & O'Donnell, M. A tale of toroids in DNA metabolism. *Nat. Rev. Mol. Cell Biol.* **1**, 22–30 (2000).

32. Horiike, K., Tojo, H., Yamano, T. & Nozaki, M. Interpretation of the Stokes radius of macromolecules determined by gel filtration chromatography. *J. Biochem.* **93**, 99–106 (1983).

33. Salmon, E.D., Saxton, W.M., Leslie, R.J., Karow, M.L. & McIntosh, J.R. Diffusion coefficient of fluorescein-labeled tubulin in the cytoplasm of embryonic cells of a sea urchin: video image analysis of fluorescence redistribution after photobleaching. *J. Cell Biol.* **99**, 2157–2164 (1984).

34. Sorger, P.K. & Pelham, H.R. Purification and characterization of a heat-shock element binding protein from yeast. *EMBO J.* **6**, 3035–3041 (1987).

35. Russell, I.D., Grancell, A.S. & Sorger, P.K. The unstable F-box protein p58-Ctf13 forms the structural core of the CBF3 kinetochore complex. *J. Cell Biol.* **145**, 933–950 (1999).